Decoupling Control of Permanent Magnet Synchronous Motor Based on Parameter Identification of Fuzzy Least Square Method

Xin Liu, Yanfei Pan, Yilin Zhu*, Hui Han, and Lei Ji

Abstract—In order to improve the performance of decoupling control for an interior permanent magnet synchronous motor (IPMSM), a recursive least square algorithm with fuzzy forgetting factor is proposed to identify IPMSM parameters. Firstly, the problems of coupling and parameter identification of IPMSM are analyzed. Secondly, the identification process of resistance and flux linkage is analyzed, and the static parameters are identified as the initial value or constant value. Thirdly, fuzzy control is used to dynamically adjust the forgetting factor in the recursive least square algorithm to make the identification of direct axis and quadrature axis inductance parameters more accurate. Finally, the effectiveness and accuracy of the proposed parameter identification algorithm are verified on the platform, and the good performance of the proposed algorithm in decoupling control is verified. The experimental results show that the identification method can accurately identify the motor parameters in static state and dynamic state. At the same time, the forgetting factor is dynamically adjusted to improve the parameter identification effect and decoupling control performance of the motor.

1. INTRODUCTION

Interior permanent magnet synchronous motor (IPMSM) has the characteristics of simple structure, reliable operation, small volume, high power density, wide speed regulation range, etc. It has been widely used in electric machines, mining industry, cranes applications, and other fields [1–4]. The IPMSM control is essentially the control of transient torque in transient process. Vector control is often used in engineering, and simple proportional integral (PI) control is used to adjust the current. However, PI current regulator often ignores the coupling effect between direct axis (d-axis) current component and quadrature axis (q-axis) current component in feedback control, which will reduce the static characteristics of IPMSM and is not conducive to the realization of vector control.

The inductance parameters of the IPMSM in conventional feed-forward decoupling control are considered as constant. However, the electrical parameters of the IPMSM change with the change of temperature and saturation degree of magnetic circuit, and it is necessary to track the change of parameters in real-time and accurately. At present, the common parameter identification algorithms are the Kalman filter method, model reference adaptive system, artificial intelligence algorithm, and recursive least square (RLS) algorithm. In [5], a Kalman filter converts the input signal into a linear system output, but it is not suitable for the nonlinear relation of actual motor system. In [6–8], the extended Kalman filter method expands the nonlinear motor model by Taylor series and omits the second-order and higher-order terms to obtain the approximate first-order linearized model, but the parameters to be identified should be treated as state quantities, and its estimation performance is limited for strong nonlinear systems. In [9–11], the difference between the output of the reference model and the adjustable model is used to realize the on-line identification of motor parameters through the appropriate adaptive law design, but it is difficult to determine the adaptive law to meet the stability

requirement when multiple parameters are identified simultaneously. In [12–15], artificial intelligence algorithm has strong nonlinear system processing ability and strong self-optimizing ability, and it has a broad application prospect in the field of PMSM parameter identification, but the complexity of the algorithm makes the algorithm limited to theoretical research. In [16], a novel internal model control approach based on the back-propagation neural network inverse control method is proposed to decouple the permanent magnet in-wheel motor, and the effectiveness of the proposed control approach is verified by means of simulation and real-time hardware-in-the-loop experiments. The RLS algorithm is widely used for on-line identification of motor parameters because of its simple objective function, moderate computation, and accurate results [17], and the forgetting factor is introduced to further improve the convergence rate and track the change of parameters in time [18]. The selection of forgetting factors is more based on experience at present. In order to solve the above problems and identify the parameters at the same time, the RLS algorithm with forgetting factor which is optimized by fuzzy algorithm is adopted to identify the parameters. In the proposed method, the resistance offline under different conditions and the amplitude of the flux linage in the initial stage of the motor operation is identified to eliminate the degenerate-rank problems, thus to ensure the accuracy of the parameter identification. The identified parameters are applied to voltage decoupling control to achieve high-performance control.

This paper consists of six sections. In Section 2, the mathematical model and parameter identification analysis of IPMSM are briefly summarized. In Section 3, firstly, the static parameters are identified as the initial value or constant value. Then, the RLS algorithm is used to dynamically identify the d- and q-axis inductors, and the forgetting factor of the RLS algorithm is dynamically adjusted by fuzzy control, so as to improve the identification accuracy of the inductor parameters. In Section 4, the correctness and effectiveness of the decoupling control based on fuzzy forgetting factor recursive least square algorithm are verified on the experimental platform. Finally, the findings of this paper are summarized in Section 6.

2. MATHEMATICAL MODEL OF THE IPMSM AND PARAMETER IDENTIFICATION ANALYSIS

According to Figure 1, the mathematical model of IPMSM in d-q axis coordinate system is

$$\begin{cases} L_d p i_d = -R_s i_d + \omega_e \psi_q + u_d \\ L_q p i_q = -R_s i_q - \omega_e \psi_d + u_q \end{cases} \tag{1}$$

$$\begin{cases} \psi_d = L_d i_d + \psi_f \\ \psi_q = L_q i_q \end{cases} \tag{2}$$

where p is the differential operator; L_d and L_q are inductances in d- and q-axes, respectively; u_d, u_q, i_d, and i_q are voltages and currents in d- and q-axes, respectively; R_s is the resistance of stator; ψ_f is the flux linkage of permanent magnet [19]; ψ_d, ψ_q are the flux linkage of stator in d- and q-axes; ω_e is the electric angular velocity of motor.

In Equations (1) and (2), the product of motor speed and the flux linkage in d- and q-axes is the coupling part. One part of the output of the PI regulator is used to counteract the back electromotive force (EMF), and the other is used to control current change in d- and q-axes. The long adjustment time leads to the decrease of the adjustment accuracy and reduces the dynamic performance. Therefore, current loop decoupling control is needed to improve the control performance.
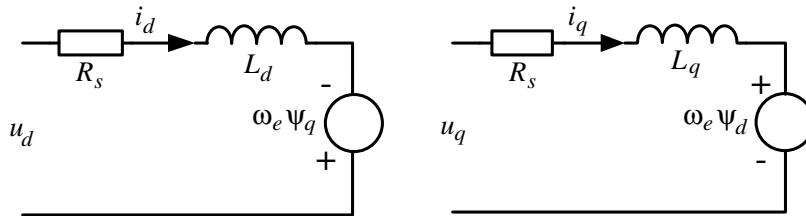

Figure 1. Equivalent model of the IPMSM in the d-q axis coordinate system.

The traditional voltage feed-forward compensation decoupling control has the advantages of simple algorithm and effective control. The expressions are

$$\begin{cases} u_d^* = u_{d0} - \omega_e L_q i_q = u_{d0} - u_{dD} \\ u_q^* = u_{q0} + \omega_e L_d i_d + \omega_e \psi_f = u_{q0} + u_{qD} \end{cases} \tag{3}$$

where u_{dD} and u_{qD} are decoupling voltages in d- and q-axes, respectively.

In Equation (3), L_d, L_q, and ψ_f change with the motor operation, so it is necessary to identify these parameters accurately. Thus, it is necessary to design the corresponding identification algorithm to identify these parameters.

In order to analyze the mathematical model, the above current formula can be rewritten as

$$\begin{bmatrix} L_d p i_d \\ L_q p i_q \end{bmatrix} = \mathbf{A} \begin{bmatrix} R_s \\ L_d \\ L_q \\ \psi_f \end{bmatrix} + \begin{bmatrix} u_d \\ u_q \end{bmatrix} \tag{4}$$

where $\mathbf{A} = \begin{bmatrix} -i_d & 0 & \omega_e i_q & 0 \\ -i_q & -\omega_e i_d & 0 & -\omega_e \end{bmatrix}$.

The second column is linearly correlated in the fourth column in the matrix $\mathbf{A}$, so L_d and ψ_f are coupled. At the same time, there are only 2 equations in Equations (1) and (2), but 4 parameters are need to be identified, so there is the problem of degenerate-rank. If we want to identify these parameters at the same time without proper convergence speed and inaccurate initial value, the misconvergence will occur because of countless suboptimal solutions. Therefore, in order to accurately identify the parameters of the IPMSM, it is necessary to obtain accurate initial parameters of the IPMSM and construct full rank expressions of the IPMSM.

The equivalent model of the IPMSM in the d-q axis coordinate system is shown in Figure 1. When the rotational speed is 0, the corresponding back EMF part is also 0, so the initial values of R_s, L_d, and L_q for the IPMSM can be obtained according to Equation (4) and equivalent model shown in Figure 1.

3. PARAMETERS IDENTIFICATION SCHEME OF THE IPMSM

3.1. Identification of Static Parameters

When the motor is at rest, the value of R_s can be obtained by injecting a constant current into the d-axis in Figure 1. For the purpose of eliminating the influence of nonlinear factors such as voltage drop in power devices, currents in d-axis with different but constant amplitudes can be injected at the same temperature, and the expressions are

$$\begin{cases} u_{d0} = i_{d0} R_s + u_{\text{offset}} \\ u_{d1} = i_{d1} R_s + u_{\text{offset}} \end{cases} \tag{5}$$

where i_{d0} and i_{d1} are the currents in d-axis with different amplitudes, u_{d0} and u_{d1} are voltages in d-axis, and u_{offset} is the voltage drop caused by nonlinear factors in power devices.

The value of R_s that is not affected by nonlinear factors can be obtained by Eq. (5), and the expression is

$$R_s = \frac{u_{d1} - u_{d0}}{i_{d1} - i_{d0}} \tag{6}$$

The value of R_s in Eq. (6) is the stator resistance at a certain temperature. The analysis of the change of stator resistance and temperature shows that they are proportional to each other, so the value of R_s at different temperatures can be obtained by injecting current into the IPMSM, and other values of R_s can be obtained by interpolated method.

After the identification of R_s is completed, AC current in the form of Eq. (7) can be injected into the IPMSM.

$$\begin{bmatrix} i_d \\ i_q \end{bmatrix} = \begin{bmatrix} I_{\text{DC}} + I_{m1} \cos(\omega t) \\ 0 \end{bmatrix} \tag{7}$$

The value of voltage is measured indirectly by voltage reconstruction of PWM wave output from inverter, and it can effectively avoid the impact of dead-time and other factors on the voltage. For the reconstructed u_d and sampled i_d, the effective values U_d and I_d of u_d and i_d, and the phase difference between u_d and i_d are calculated more efficiently by using discrete Fourier transform (DFT) than fast Fourier transform (FFT) because the frequency of the injected current is known, and then the L_d can be calculated by Equation (8).

$$L_d = \frac{\sqrt{Z_d^2 - R_s^2}}{\omega} \tag{8}$$

where Z_d is the reactance in d-axis; the value is U_d/I_d; ω is the frequency of the current injected into the d-axis; R_s is the stator resistance identified by Equation (6).

Similarly, the value of L_q can be identified by injecting the AC current into the IPMSM, and the added DC component I_{DC} can maintain rotor stable and reduce vibration noise.

$$\begin{bmatrix} i_d \\ i_q \end{bmatrix} = \begin{bmatrix} I_{DC} \\ I_{m2} \cos(\omega t) \end{bmatrix} \tag{9}$$

So far, the parameters such as R_s, L_d, and L_q can be identified when the motor is static, and the ψ_f can be obtained according to the nameplate parameters. Then, the IPMSM can carry out vector control accurately and efficiently. Only relying on the values of L_d and L_q identified by static cannot realize the control of the IPMSM accurately and efficiently. In order to obtain more accurate parameters such as L_d, L_q, and ψ_f, it is necessary to update constantly.

When the IPMSM is in operation, there are three parameters to be identified, i.e., L_d, L_q, and ψ_f. Without additional information, we can see that the equation with rank 2 cannot accurately identify the three parameters. Therefore, the identification process needs additional processing.

When the motor is started with $i_d = 0$ and running to a certain speed and running stably for a period of time, the value of ψ_f can be calculated according to Figure 1 and Equation (10).

$$\psi_f = \frac{u_q - R_s i_q}{\omega_e} \tag{10}$$

When the identification of ψ_f is completed, switch the control mode to maximum torque per ampere (MTPA) mode, according to R_s, L_d, L_q, and ψ_f identified at rest, and the distribution of current and the decoupling of voltage are more accurate. Therefore, in order to obtain higher control bandwidth and better decoupling control performance, it is necessary to identify L_d and L_q which change greatly with the working conditions.

3.2. Algorithm of Dynamic Parameter Identification

3.2.1. Recursive Least Square Algorithm

For an observable system, L sets of input-output observations can be expressed as $\{y(k), u(k), k = 1, 2, ..., L\}$, and the LS estimation $\hat{\theta}$ of system parameters can be obtained by batch processing.

$$\hat{\theta} = \left(\Phi^T \Phi\right)^{-1} \Phi^T \mathbf{Y} \tag{11}$$

where Φ is the data vector matrix, and $\mathbf{Y}$ is the output matrix of system.

In the application of batch processing to calculate the LS algorithm, the large amount of data per processing not only occupies a large amount of memory, but also cannot estimate the parameters in real-time, so the RLS method can be used to solve these problems. The basic idea of RLS algorithm is

$$\hat{\theta}(k) = \hat{\theta}(k-1) + \{\text{correction term}\}$$

The LS estimation at the k time by batch processing is

$$\hat{\theta}(k) = \left(\Phi_k^T \Phi_k\right)^{-1} \Phi_k^T \mathbf{Y}_k \tag{12}$$

where $\Phi_k = \begin{pmatrix} \Phi_{k-1} \\ \varphi^T(k) \end{pmatrix} \in \mathbf{R}^{k \times (n_a + n_b + 1)}$, $\mathbf{Y}_k = \begin{pmatrix} \mathbf{Y}_{k-1} \\ y(k) \end{pmatrix} \in \mathbf{R}^{k \times 1}$.

Let covariance matrix $\mathbf{P}(k)$ be

$$\mathbf{P}(k) = \left(\mathbf{\Phi}_k^T\mathbf{\Phi}_k\right)^{-1} = \left[\mathbf{\Phi}_{k-1}^T\mathbf{\Phi}_{k-1} + \varphi(k)\varphi^T(k)\right]^{-1} = \left[\mathbf{P}^{-1}(k-1) + \varphi(k)\varphi^T(k)\right]^{-1} \tag{13}$$

Then

$$\mathbf{P}^{-1}(k) = \mathbf{P}^{-1}(k-1) + \varphi(k)\varphi^T(k) \tag{14}$$

From Equations (12), (13), and (14), the estimated value at the $k-1$ time can be calculated as

$$\hat{\boldsymbol{\theta}}(k-1) = \left(\mathbf{\Phi}_{k-1}^T\mathbf{\Phi}_{k-1}\right)^{-1}\mathbf{\Phi}_{k-1}^T\mathbf{Y}_{k-1} = \mathbf{P}(k-1)\mathbf{\Phi}_{k-1}^T\mathbf{Y}_{k-1} \tag{15}$$

From Equations (14) and (15)

$$\mathbf{\Phi}_{k-1}^T\mathbf{Y}_{k-1} = \mathbf{P}^{-1}(k-1)\hat{\boldsymbol{\theta}}(k-1) = \left[\mathbf{P}^{-1}(k-1) + \varphi(k)\varphi^T(k)\right]\hat{\boldsymbol{\theta}}(k-1) \tag{16}$$

The LS estimation at the k time is

$$\hat{\boldsymbol{\theta}}(k) = \mathbf{P}(k)\mathbf{\Phi}_k^T\mathbf{Y}_k = \hat{\boldsymbol{\theta}}(k-1) + \mathbf{K}(k)\left[y(k) - \varphi^T(k)\hat{\boldsymbol{\theta}}(k-1)\right] \tag{17}$$

where $K(k)$ is the gain matrix, $\mathbf{K}(k) = \mathbf{P}(k)\varphi(k)$.

The iterative formula of RLS algorithm can be obtained from matrix inverse theory and Equation (17).

$$\begin{cases} \hat{\boldsymbol{\theta}}(k) = \hat{\boldsymbol{\theta}}(k-1) + \mathbf{K}(k)\left[y(k) - \varphi^T(k)\hat{\boldsymbol{\theta}}(k-1)\right] \\ \mathbf{K}(k) = \dfrac{\mathbf{P}(k-1)\varphi(k)}{1 + \varphi^T(k)\mathbf{P}(k-1)\varphi(k)} \\ \mathbf{P}(k) = \left[I + \mathbf{K}(k)\varphi^T(k)\right]\mathbf{P}^{-1}(k-1) \end{cases} \tag{18}$$

When the recursive formula is used for parameter identification, we need to determine the initial value of the covariance matrix and the identified parameters, and the following two methods are generally used.

1) If L sets of data $(L > n_a + n_b + 1)$ have been obtained, use the batch least square method to calculate

$$\begin{cases} \mathbf{P}(L) = \left(\mathbf{\Phi}_L^T\mathbf{\Phi}_L\right)^{-1} \\ \hat{\boldsymbol{\theta}}(L) = \left(\mathbf{\Phi}_L^T\mathbf{\Phi}_L\right)^{-1}\mathbf{\Phi}_L^T\mathbf{Y}_L \end{cases} \tag{19}$$

2) Set

$$\begin{cases} \mathbf{P}(0) = \alpha\mathbf{I} \\ \hat{\boldsymbol{\theta}}(0) = \sigma \end{cases} \tag{20}$$

where α is a fully large positive real number and σ a zero vector or a fully small positive real vector.

3.2.2. Recursive Least Square Algorithm with Fuzzy Forgetting Factor

With the increase of processing data, the data of RLS algorithm will saturate, so the forgetting factor is adopted. However, the forgetting factor in the traditional RLS algorithm is fixed and cannot be adjusted best according to the real-time performance. Therefore, the forgetting factor can be fuzzified by fuzzy control theory, and an appropriate forgetting factor can be obtained by existing experience. Revise the performance indicator as

$$J = \sum_{k=1}^{L}\lambda^{L-k}\left[y(k) - \varphi^T(k)\hat{\boldsymbol{\theta}}\right]^2 \tag{21}$$

where λ is the forgetting factor, $0 < \lambda \leq 1$.

Therefore, Equation (18) can be rewritten as

$$\begin{cases} \hat{\boldsymbol{\theta}}(k) = \hat{\boldsymbol{\theta}}(k-1) + \mathbf{K}(k)\left[y(k) - \varphi^T(k)\hat{\boldsymbol{\theta}}(k-1)\right] \\ \mathbf{K}(k) = \dfrac{\mathbf{P}(k-1)\varphi(k)}{\lambda + \varphi^T(k)\mathbf{P}(k-1)\varphi(k)} \\ \mathbf{P}(k) = \dfrac{1}{\lambda}\left[I + \mathbf{K}(k)\varphi^T(k)\right]\mathbf{P}^{-1}(k-1) \end{cases} \tag{22}$$

The value range of forgetting factor is usually selected as $0.9 \leq \lambda \leq 1$, so the forgetting factor can be fuzzified according to the error.

Define the error as

$$\mathbf{e} = \mathbf{y}(k) - \boldsymbol{\varphi}^T(k)\hat{\boldsymbol{\theta}}(k-1) \tag{23}$$

The error $\mathbf{e}$ is a two-dimensional vector and is used as the input variable of the fuzzy controller to adjust the forgetting factor λ, and the forgetting factor λ is used as the output variable of the fuzzy controller. The closer the forgetting factor is to 0, the faster the convergence rate is, but the stability will be affected. Therefore, when the parameters are stable, the forgetting factor is gradually increased to improve the stability of the algorithm.

1) fuzzification

Several linguistic labels are used to describe the fuzzy sets of two inputs and one output, namely, zero (Z), positive small (PS), positive middle (PM), and positive big (PB). In this paper, set the fuzzy domain of two error $\mathbf{e}$ as $[0, 3]$; set the fuzzy subset as {Z, PS, PM, PB}; the practical domain of $\mathbf{e}$ and quantization factor are determined according to error parameters. The output variable of fuzzy controller is forgetting factor λ; set the fuzzy domain is $[0.9, 1]$; set the fuzzy subset as {PS, PM, PB}. According to the actual control effect, actual values of K can be quantified. To simplify the calculation, the input and output variables obey the triangular membership function distribution curve, and the distribution curve is shown in Figure 2.
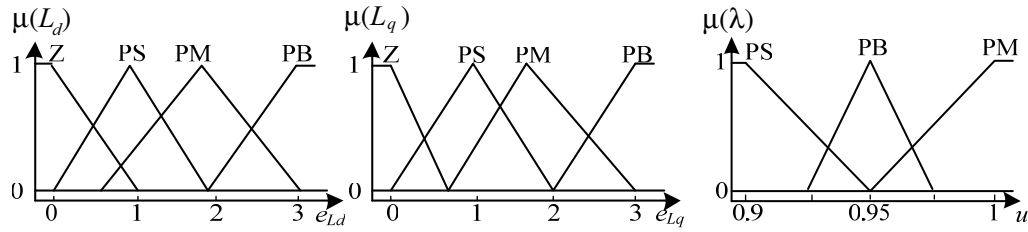

Figure 2. Input-output membership function diagram.

Figure 2 shows the membership functions of the inputs and output adopted according to the experimental results. The membership functions map the crisp value of inputs and output to the membership μ of each fuzzy set.

2) Fuzzy Rule Base and Reasoning

Fuzzy rule base is composed of multiple IF-THEN rules with antecedents and consequent parts. The rules are $R_{i,j}$: If e_{Ld} is E_{Ldi} and e_{Lq} is E_{Lqj}, u is U_m, where $i, j = 1, 2, 3, 4$; $m = 1, 2, 3$.

For example, $R_{1,1}$: If e_{Ld} is Z and e_{Lq} is Z, λ is PB; $R_{4,4}$: If e_{Ld} is PB and e_{Lq} is PB, λ is PS.

All the control rules can be expressed more clearly through a 4×4 matrix, which are listed in Table 1.

Table 1. Rule base of fuzzy logic.

λ		e_{Ld}			
		Z	PS	PM	PB
e_{Lq}	Z	PB	PB	PM	PM
	PS	PB	PM	PM	PS
	PM	PM	PM	PM	PS
	PB	PM	PS	PS	PS

The inference block aggregates all the IF-THEN rules with their weighting factors according to the input fuzzy sets e_{Ld} and e_{Lq}. The weighting factor of each rule $\omega_{i,j}$ is obtained by product operation and can be expressed as

$$\omega_{i,j} = \mu(L_d) \cdot \mu(L_q) \tag{24}$$

3) Defuzzication

In order to obtain smooth output, the center of gravity method is used to get the output defuzzification results.

$$u = \left(\sum_{i=1}^{4} \sum_{i=1}^{4} \omega_{i,j} u_{i,j} \right) \Big/ \left(\sum_{i=1}^{4} \sum_{i=1}^{4} \omega_{i,j} \right) \tag{25}$$

where $u_{i,j}$ is the clear value of the output fuzzy set corresponding to each control rule.

Because of the triangular membership function is adopted, the denominator in Equation (25) can be transformed into

$$\sum_{i=1}^{4} \mu(L_d) = 1, \quad \sum_{i=1}^{4} \mu(L_q) = 1 \tag{26}$$

Combined with Equations (24), (25), and (26), the output can be rewritten as

$$u = \sum_{i=1}^{4} \sum_{i=1}^{4} \omega_{i,j} u_{i,j} \tag{27}$$

The RLS algorithm with forgetting factor based on fuzzy control (FRLS) has been completed, and the control block diagram of the whole identification is shown in Figure 3.
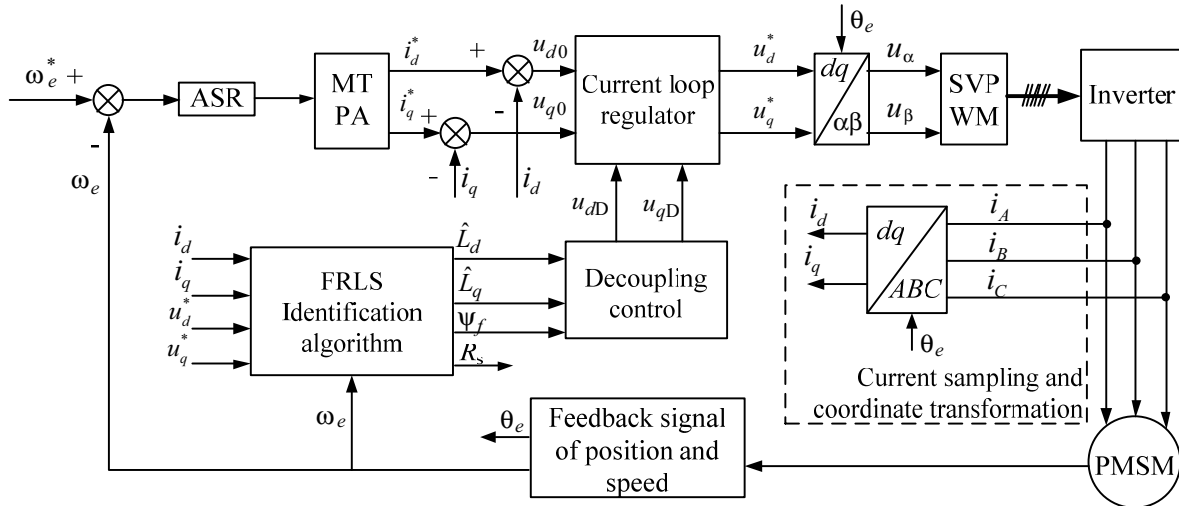
Figure 3. Decoupling control block diagram with parameter identification.

4. EXPERIMENTAL VERIFICATION

In order to verify the validity and correctness of the proposed method, experimental verification is carried out on the experimental platform shown in Figure 4, and the experimental parameters of the prototype are shown in Table 2. It consists of electric dynamometer, torque and speed sensor, IPMSM, control board, oscilloscope, and computer. PI controllers are used in automatic speed regulator (ASR) and automatic current regulator (ACR). The ASR parameter is set as $k_p = 1.00$, $k_i = 0.0002$, the ACR parameter in d-axis set as $k_p = 0.23$, $k_i = 0.002$, and the ACR parameter in q-axis set as $k_p = 0.69$, $k_i = 0.002$.

The stator resistance is identified at first, and different currents are injected in d-axis to obtain the voltages at different times and temperatures, record and store them. After calculation, the fitting formula is $R_s = 13.92 \times 10^{-6}T + R_0$, where T is the motor temperature, whose unit is $°$.

When the motor is static, the currents shown in Equations (7) and (9) are injected into the motor, and data acquisition and processing are completed. By calculation, the initial identification of d- and
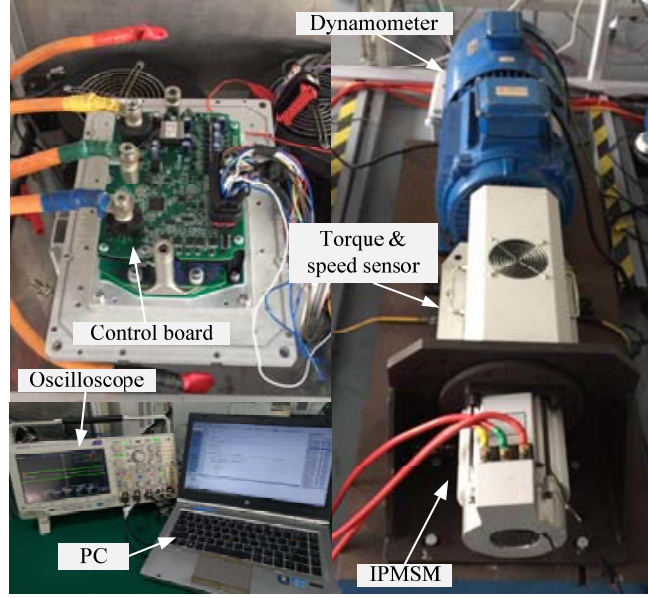
Figure 4. Experimental platform.

Table 2. IPMSM parameters.

Parameter	Value
Stator resistance R_s/Ω	0.006
Stator inductance $L_d/\mu H$	68.3
Stator inductance $L_q/\mu H$	189.0
Pole-pair numbers	4
Rated voltage u_{dc}/V	96
Flux linkage of permanent magnet ψ_f/Wb	0.03
Rated power P/kW	20
Rated current I/A	190
Rated torque $T_e/(N \cdot m)$	54
Rated speed $n/(rpm)$	3600
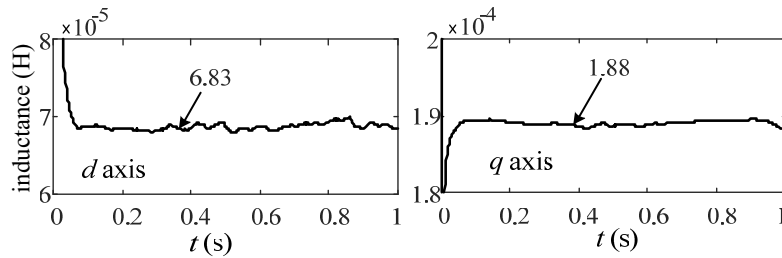
Figure 5. The waveform of d- and q-axis inductances when the motor at rest.

q-axis inductances is completed. Figure 5 shows the d- and q-axis inductances when the motor is at rest, and the values are 68.3 μH and 188.0 μH, respectively. The identification values fluctuate slightly within the acceptable range, and the value is basically consistent with the theoretical value in Table 2.
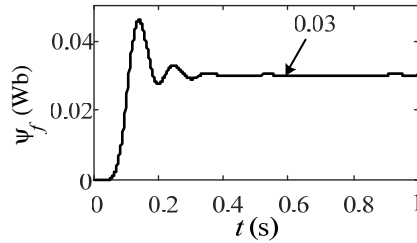
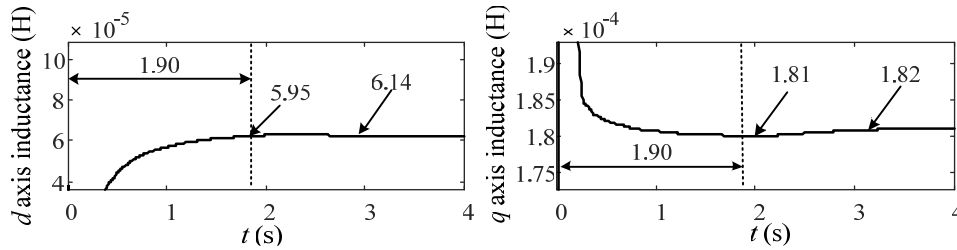**Figure 6.** The waveform of flux linkage value.

Figure 7. The waveforms d- and q-axis inductance identified by the traditional RLS algorithm.
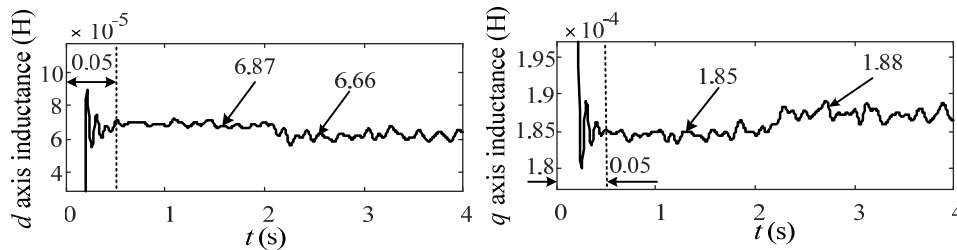

Figure 8. The waveforms d- and q-axis inductance identified by the RLS algorithm with fuzzy forgetting factor.

Figure 6 shows the flux linkage identified by Equation (10) when the motor is in the initial operation. In Figure 6, when the flux value reaches stability, the value is stable at 0.03 Wb which is consistent with the theoretical value, and it indicates that the method can effectively obtain the initial flux value.

Figure 7 shows the waveforms of d- and q-axis inductances identified by the traditional RLS algorithm. The motor runs at a load torque of 1 N·m before 2 s and then at 50% rated torque after 2 s, and the value is 27 N·m. In Figure 7, the inductance identification values in d-axis are 59.5 µH and 61.4 µH, respectively, and the inductance identification values in q-axis are 181.0 µH and 182.0 µH, respectively, which are a slight deviation from the theoretical values in Table 2. Figure 8 shows the waveforms of d- and q-axis inductances identified by the RLS algorithm with fuzzy forgetting factor. The motor runs at a load torque of 1 N·m before 2 s and then at 50% rated torque after 2 s, and the value is 27 N·m. In Figure 8, the inductance identification values in d-axis are 68.7 µH and 66.6 µH, respectively, and the inductance identification values in q-axis are 185.0 µH and 188.0 µH, respectively, which have a slight deviation from the theoretical value in Table 2, but the deviation is smaller than that of the traditional LS algorithm. The convergence time of the LS algorithm with fuzzy forgetting factor is 0.05 s, while that of the traditional least square method is 1.90 s, which indicates that the proposed method has a faster convergence speed, but the problem of jitter still exists. Although the jitter of identification result of the proposed method is larger than that of the traditional LS algorithm, the jitter amplitude is within the acceptable range.

Figure 9 shows the waveforms of d- and q-axis currents without voltage feed-forward decoupling. In Figure 9, when the current reaches a steady state, it needs 0.034 s, and the maximum amplitude of the d- and q-axis currents reach -110 A and 184 A.
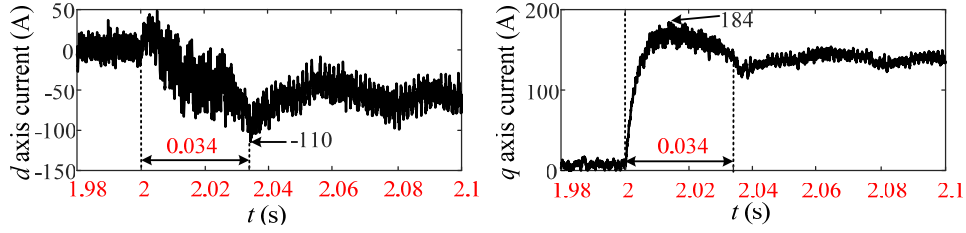
Figure 9. The waveforms of d- and q-axis current without voltage feed-forward decoupling.
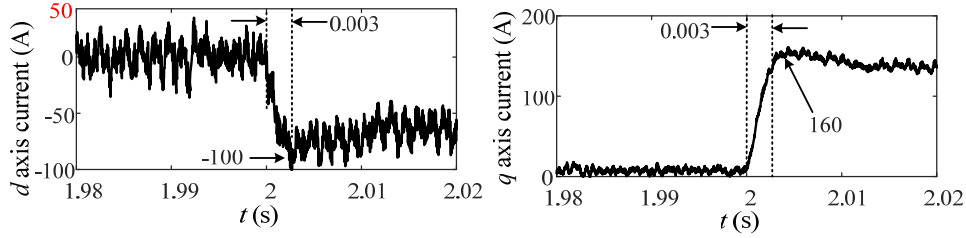

Figure 10. The waveforms of d- and q-axis current of voltage feed-forward decoupling control with traditional RLS algorithm.
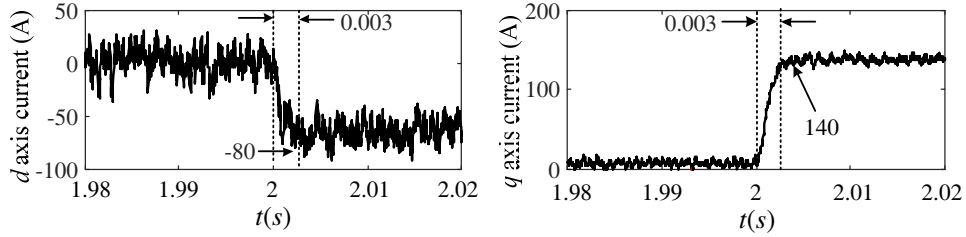

Figure 11. The waveforms of d- and q-axis current of voltage feed-forward decoupling control with fuzzy forgetting factor RLS algorithm.

Figure 10 shows the waveforms of d- and q-axis currents of voltage feed-forward decoupling control with traditional RLS algorithm. In Figure 10, when the current reaches a steady state, it needs 0.003 s, and the maximum amplitudes of the d- and q-axis currents reach -100 A and 160 A.

Figure 11 shows the waveforms of d- and q-axis currents of voltage feed-forward decoupling control with fuzzy forgetting factor RLS algorithm. In Figure 11, when the current reaches steady state, it needs 0.003 s, and the maximum amplitudes of the d- and q-axis currents reach -80 A and 140 A.

From Figures (9) to (11), when the voltage feed-forward decoupling control is adopted, the current response time is reduced from 0.03 s to 0.003 s, and the response time is greatly improved. The current amplitude is also gradually reduced. In the decoupling control of the traditional RLS algorithm identification parameters, there is still a small coupling of the d- and q-axis currents, but when the proposed method is adopted in this paper, the coupling of the d- and q-axis currents is improved.

5. CONCLUSIONS

In order to improve the performance of the decoupling control and solve degenerate-rank problems caused by identifying the resistance, inductance, and flux linkage at the same time, the resistance is identified offline under different conditions, and the amplitude of the flux linage is identified in the initial stage of the motor operation, then the RLS algorithm with forgetting factor is adopted to identify the inductance, and the forgetting factor in the identification process is dynamically adjusted by fuzzy control method, so as to improve the performance of parameter identification. Firstly, the initial value of

motor inductance is obtained by calibration and off-line, and the identification results are accurate and consistent with the theoretical results. After that, the motor is operated in the control mode of $i_d = 0$, and the flux linkage of permanent magnetic is obtained accurately and quickly, and switched to normal operation quickly when the identification is completed. Finally, in order to overcome the problem of a fixed forgetting factor in traditional RLS algorithm with forgetting factor, fuzzy control is used to improve the identification performance of RLS algorithm, and it is used in real-time decoupling control after identification. The experimental results show that the proposed method has higher identification accuracy and better decoupling control performance than the traditional RLS algorithm.

REFERENCES

1. Yin, S. and W. Wang, "Study on the flux-weakening capability of permanent magnet synchronous motor for electric vehicle," *Mechatronics*, Vol. 38, 115–120, 2016.

2. Liu, G., G. Qiu, S. Jin, and F. G. Zhang, "Study on counter-rotating dual-rotor permanent magnet motor for underwater vehicle propulsion," *IEEE Transactions on Applied Superconductivity*, Vol. 28, No. 3, 1–5, 2018.

3. Zhang, B., Q. Li, G. Feng, B. Wang, and H. Sun, "Study on mine hoist driven by PMSM of low voltage and multi-branch," *Advanced Materials Research*, Vol. 2140, 22–25, 2013.

4. Knypiński, Ł. and J. Krupiński, "The slewing drive system for tower crane with permanent magnet synchronous motor," *Archives of Electrical Engineering*, Vol. 70, No. 1, 189–201, 2021.

5. Aubert, B., J. Regnier, S. Caux, and D. Alejo, "Kalman-filter-based indicator for online interturn short circuits detection in permanent-magnet synchronous generators," *IEEE Transactions on Industrial Electronics*, Vol. 62, No. 3, 1921–1930, 2015.

6. She, Z., J. Liu, Q. Liang, and W. Zou, "Identification for PMSM rotor speed based on optimized extended kalman filter and load torque observer," *2020 IEEE International Conference on Applied Superconductivity and Electromagnetic Devices (ASEMD)*, 1–2, Tianjin, China, 2020.

7. Shi, Y., "Online identification of permanent magnet flux based on extended kalman filter for IPMSM drive with position sensorless control," *IEEE Transactions on Industrial Electronics*, Vol. 59, No. 11, 4169–4178, 2012.

8. Cheng, L., X. J. Ye, D. R. Sun, Y. Ye, and Y. Jin, "Low speed compound direct-drive permanent magnet synchronous motor control system with load torque compensation," *Applied Mechanics & Materials*, Vols. 416–417, 652–657, 2013.

9. Zhong, C. and Y. Lin, "Model reference adaptive control (MRAC)-based parameter identification applied to surface-mounted permanent magnet synchronous motor," *International Journal of Electronics*, Vol. 104, No. 11, 1854–1873, 2017.

10. Qu, Z. Y. and Z. M. Ye, "Speed regulation of a permanent magnet synchronous motor via model reference adaptive control," *Advanced Materials Research*, Vols. 268–270, 513–516, 2011.

11. Kesavan, P. and A. Karthikeyan, "Electromagnetic torque-based model reference adaptive system speed estimator for sensorless surface mount permanent magnet synchronous motor drive," *IEEE Transactions on Industrial Electronics*, Vol. 67, No. 7, 5936–5947, 2020.

12. Aliprantis, D. C., S. D. Sudhoff, and B. T. Kuhn, "Genetic algorithm-based parameter identification of a hysteretic brushless exciter model," *IEEE Transactions on Energy Conversion*, Vol. 21, No. 1, 148–154, 2006.

13. Gaur, P., B. Singh, and A. Mittal, "Artificial neural network based controller and speed estimation of permanent magnet synchronous motor," *2008 Joint International Conference on Power System Technology and IEEE Power India Conference*, 1–6, New Delhi, India, 2008.

14. Sandre-Hernandez, O., R. Morales-Caporal, J. Rangel-Magdaleno, and H. Peregrina-Barreto, "Parameter identification of PMSMs using experimental measurements and a PSO algorithm," *IEEE Transactions on Instrumentation & Measurement*, Vol. 64, No. 8, 2146–2154, 2015.

15. Liu, Z. H., H. L. Wei, X. H. Li, and K. Liu, "Global identification of electrical and mechanical parameters in PMSM drive based on dynamic self-learning PSO," *IEEE Transactions on Power Electronics*, Vol. 33, No. 12, 10858–10871, 2018.

16. Li, Y., B. Zhang, and X. Xu, "Decoupling control for permanent magnet in-wheel motor using internal model control based on back-propagation neural network inverse system," *Bulletin of the Polish Academy of Sciences: Technical Sciences*, Vol. 66, No. 6, 1–12, 2018.

17. Zhang, J. L. and C. S. Zhang, "Parameters identification of induction motor for electric vehicle based on least squares method," *Advanced Materials Research*, Vols. 383–390, 648–653, 2011.

18. Zhou, Y., H. Wang, and J. Lian, "Research on online parameter identification of interior permanent magnet synchronous motor based on augmented robust forgetting factor recursive least square," *Transactions on Emerging Telecommunications Technologies*, Vol. 31, No. 12, 1–13, 2020.

19. Léopold, S., F. Maurice, P. Maria, and P. Guillaume, "MTPV flux-weakening strategy for PMSM high speed drive," *IEEE Transactions on Industry Applications*, Vol. 54, No. 6, 6081–6089, 2018.